Self-force in Hyperbolic Scattering: a Frequency Domain Approach

Chris Whittall
Supervisor: Leor Barack

25th CAPRA Meeting
22nd June 2022

Scatter orbits as strong-field probe of GR

Scatter angle defined by

$$\begin{aligned}\delta\varphi &:= \varphi_{out} - \varphi_{in} - \pi \\ &= \delta\varphi^{(0)} + \eta\delta\varphi^{(1)} + \eta^2\delta\varphi^{(2)} + \dots\end{aligned} \tag{1}$$

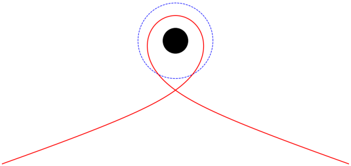

Motivations:

- Conservative PM dynamics can be inferred from self-force scatter calculations, valid at *all* mass ratios. [Damour 2020]
- Benchmarking PM results in the strong-field regime.
- Strong-field probe of GR potential.
- Comparisons with quantum amplitude methods.
- Calibrate effective-one-body models.
- Hence inform an accurate universal model of BBH inspirals, suitable for GW searches.

Frequency domain

- FD codes exist to calculate first-order GSF along generic bound Kerr geodesics [Van de Meent 2017]. Several challenges when moving to unbound orbits.
- Despite this, we are interested in frequency-domain methods due to potentially higher precision and efficiency.
- We work with **scalar field toy model** in Schwarzschild to investigate problems and solutions:
  - Continuous spectra
  - UV problem near the particle
  - Slowly convergent radial integrals

Field equation

The scalar field equation is given by

$$\nabla_\mu \nabla^\mu \Phi = -4\pi T \tag{2}$$

and the scalar charge density T is that of a point particle. We separate into spherical and Fourier harmonics:

$$\Phi = \int d\omega \sum_{\ell,m} \frac{1}{r} \psi_{\ell m\omega} Y_{\ell m}(\theta, \varphi) e^{-i\omega t}, \tag{3}$$

and the equation of motion becomes

$$\frac{d^2\psi_{\ell m\omega}}{dr_*^2} - (V_\ell(r) - \omega^2)\psi_{\ell m\omega} = S_{\ell m\omega}(r). \tag{4}$$

Inhomogeneous solution

For $\omega \neq 0$ variation of parameters gives us the inhomogeneous field

$$\psi_{\ell m\omega}(r) = \psi^{+}_{\ell m\omega}(r) \int_{r_{min}}^{r} \frac{\psi^{-}_{\ell m\omega}(r')S_{\ell m\omega}(r')}{W_{\ell m\omega}} \frac{dr'}{f(r')} + \psi^{-}_{\ell m\omega}(r) \int_{r}^{\infty} \frac{\psi^{+}_{\ell m\omega}(r')S_{\ell m\omega}(r')}{W_{\ell m\omega}} \frac{dr'}{f(r')}, \tag{5}$$

where for $\omega \neq 0$ the homogeneous solutions $\psi^{\pm}_{\ell m\omega}$ are defined by BCs:

$$\psi^{-}_{\ell m\omega}(r) \sim e^{-i\omega r_*} \quad \text{as } r_* \longrightarrow -\infty \tag{6}$$

$$\psi^{+}_{\ell m\omega}(r) \sim e^{+i\omega r_*} \quad \text{as } r_* \longrightarrow +\infty. \tag{7}$$

Extended homogeneous solutions

- Delta function source causes slow, non-uniform convergence of Fourier series/integral near the worldline (Gibbs phenomenon).

- MEHS: express time domain field $\Phi_{lm}(t,r)$ in terms of analytic functions on either side of the worldline.

$$r\Phi_{\ell m}(t,r) = \tilde{\psi}^{+}_{\ell m}(t,r)\Theta(r - r_p(t)) + \tilde{\psi}^{-}_{\ell m}(t,r)\Theta(r_p(t) - r). \tag{8}$$

  [Barack, Ori, Sago 2008]

- For bound orbit,

$$\tilde{\psi}^{\pm}_{\ell m\omega}(r) := \psi^{\pm}_{\ell m\omega}(r)\int_{r_{min}}^{r_{max}} \frac{\psi^{\mp}_{\ell m\omega}(r')S_{\ell m\omega}(r')dr'}{W_{\ell m\omega}f(r')}. \tag{9}$$

EHS: unbound case

- EHS method relies on the existence of vacuum regions $r \geq r_{max}$ and $r \leq r_{min}$ where the EHS and physical fields coincide.
- Agreement throughout the domain is deduced using an analyticity argument.
- For the unbound case, we no longer have the $r \geq r_{max}$ vacuum region. But we do still have the vacuum region $r \leq r_{min}$.
- Attempts to apply a (modified) form of EHS outside the orbit have not been successful so far.

We can only use EHS to reconstruct the field **inside** the orbit.

Slowly converging radial integrals

$$C^{-}_{\ell m\omega} := \int_{r_{min}}^{+\infty} \frac{\psi^{+}_{\ell m\omega}(r)\cos[\omega t_p(r) - m\varphi_p(r)]}{r|u^r(r)|} dr. \tag{10}$$

- Integrand singular at r_{min}. Split integration region and use integration variable χ near periapsis, r at distance.
- The integrand behaves like oscillations/r at large r. Hence we have to integrate out to great distance to get convergence.
- At higher frequencies, need to integrate over many wavecycles, at great cost. A single integral can take $> 30s$ if done naively.

Truncating the integral: problems

- Truncating at such radii causes issues in the tail of the spectrum.
- Suppressing this requires r_{max} to increase by orders of magnitude. Not feasible due to runtime cost.
- Need to increase decay rate, speed up integration, or approximate tail. All are possible.

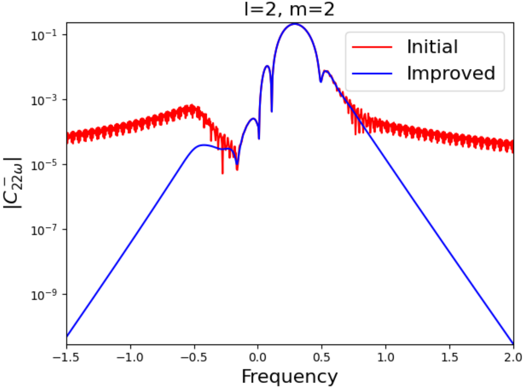

Figure: Red curve shows effect of truncating integral at $r_{max} = 1980M$. With new techniques, we obtain an improved spectrum

Analytical approximations to the tail: theory

The integrand of $C^{-}_{\ell m\omega}$,

$$J_{\ell m\omega}(r) = \frac{1}{2}\sum_{\sigma=\pm1} \frac{\psi^{+}_{\ell lm\omega}(r')\exp\left[i\sigma\left(\omega t_p(r') - m\varphi_p(r')\right)\right]}{r'\left|u^r(r')\right|}, \qquad (11)$$

has a series expansion as $r \to \infty$:

$$J_{\ell m\omega}(r) = \frac{1}{2\sqrt{E^2-1}} \sum_{\sigma=\pm1}\sum_{n\geq 0} e^{i\sigma\Delta^{(0)}_{\infty}} \lambda^{(n)}_{\sigma} e^{i\omega(1+\sigma A)r}\, r^{i(1+\sigma B)\omega-1-n}, \qquad (12)$$

where $A, B, \Delta^{(0)}_{\infty}$ and $\lambda^{(n)}_{\sigma}$ are constants. Thus

$$\int_{r_{max}}^{+\infty} J_{\ell m\omega}(r)dr \approx \frac{1}{2\sqrt{E^2-1}} \sum_{\sigma=\pm1}\sum_{n=0}^{N} \lambda^{(n)}_{\sigma} e^{i\sigma\Delta^{(0)}_{\infty}} r^{a}_{max} z^{-a}\Gamma[a,z], \qquad (13)$$

where $a = i(1+\sigma B)\omega - n$ and $z = -\omega(1+\sigma A)r_{max}$.

Analytical approximations to the tail: impact

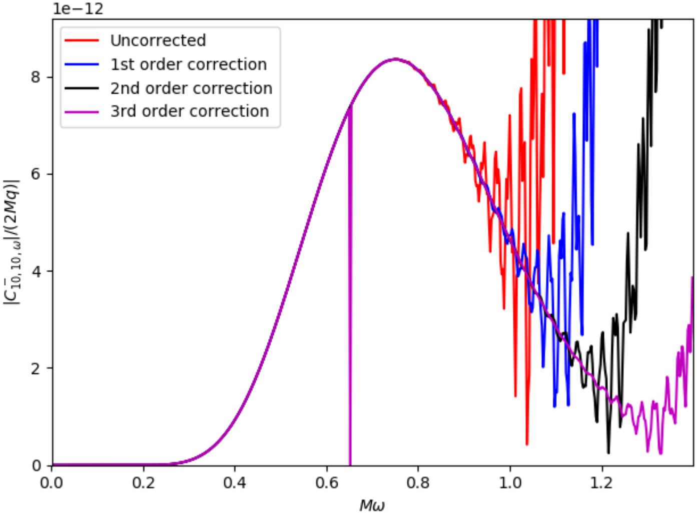

Have corrections up to 6th order, but this is not enough.

Integration by parts (1)

Integration by parts can be used to increase the rate of convergence.

We can rewrite the integrand

$$J_{\ell m\omega}(r) := \frac{1}{2}\sum_{\sigma=\pm 1} e^{i\Omega_\sigma r} K^{\sigma}_{\ell m\omega}(r), \tag{14}$$

where $\Omega_\sigma := \omega(1+\sigma/v)$ and the function $K^{\sigma}_{\ell m\omega}$ has the asymptotics

$$K^{\sigma}_{\ell m\omega} \sim r^{i\omega(1+\sigma B)-1} \tag{15}$$

as $r \to \infty$. Then we have the property

$$\frac{d^N K^{\sigma}_{\ell m\omega}}{dr^N} = O\left(\frac{1}{r^{N+1}}\right) \tag{16}$$

as $r \to \infty$.

Integration by parts (2)

Applying integration by parts $N+1$ times,

$$C^{-(r)}_{\ell m\omega} = \frac{1}{2}\sum_{\sigma=\pm 1}\left\{\sum_{n=0}^{N}\left[\left(\frac{i}{\Omega_\sigma}\right)^{n+1} e^{i\Omega_\sigma r_{cut}} K^{\sigma(n)}_{\ell m\omega}(r_{cut})\right] + \left(\frac{i}{\Omega_\sigma}\right)^{N+1}\int_{r_{cut}}^{+\infty} e^{i\Omega_\sigma r} K^{\sigma(N+1)}_{\ell m\omega}(r)dr\right\}. \quad (17)$$

Integration by parts can be applied as many times as required. Limited only by need to derive expressions for the derivatives $K^{\sigma(n)}_{\ell m\omega}$.

We have implemented 4 iterations of IBP, i.e. truncation error $O(r_{max}^{-5})$.

Oscillatory quadrature

- IBP slightly reduces time cost, but $C^{-}_{\ell m\omega}$ can still take $O(10s)$ to calculate at high ω.
- Clenshaw-Curtis quadrature suited to integrals with a sine/cosine weight function. Easily applied to our integrand in the form $e^{i\Omega_\sigma r} K^{\sigma(n)}_{\ell m\omega}$.
- Reduces runtime to 1-2s for a single integral, increasing only slowly with ω.
- Faster quadrature means one can integrate out to larger r_{max} in given time, or reach the same r_{max} in a smaller time.

Improved spectrum

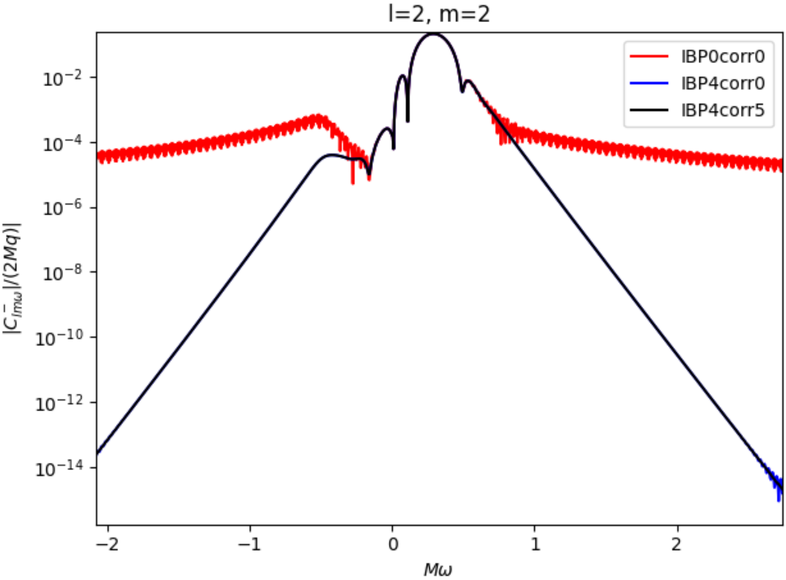

Time-domain reconstruction

Efficiency: in bound case we can save time by reusing $C^{-}_{\ell mn}$ values.

Options for time-domain reconstruction with *continuous* spectrum:

1. Adaptive integration, calculating $C^{-}_{\ell m\omega}$ on-the-fly:
   - Good control over error, cannot reuse frequencies
2. Fixed point integration, with $C^{-}_{\ell m\omega}$ at pre-generated frequencies:
   - Can re-use frequencies, no control over error
3. Pre-generate $C^{-}_{\ell m\omega}$ at given frequencies, then use adaptive integration and interpolation:
   - Can re-use frequencies, good control over error, interpolation may be less accurate than direct numerical calculation of $C^{-}_{\ell m\omega}$

Used (1) for initial testing, but now use (3).

Self-force calculation: t-component (1)

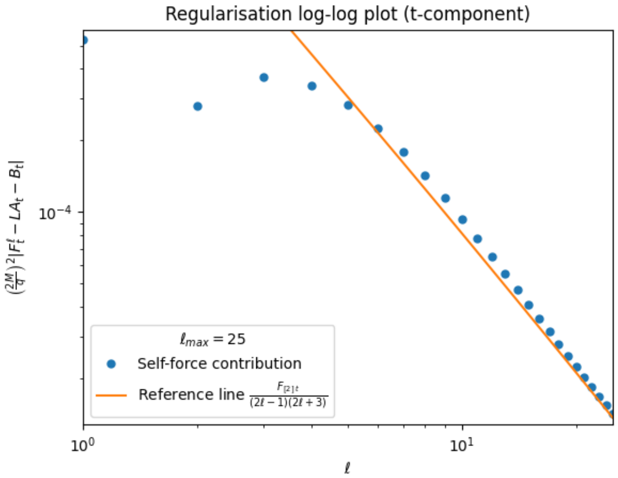

Calculation of the self-force passes initial regularisation tests

Self-force calculation: t-component (2)

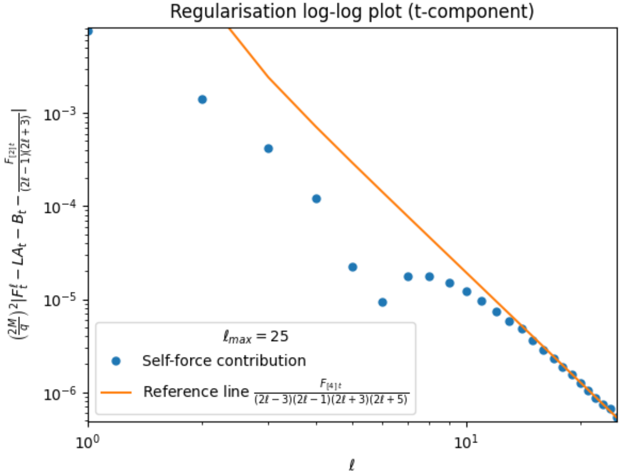

Can subtract higher order parameters.

Self-force calculation: other components

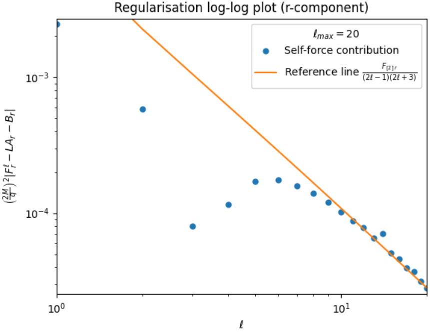

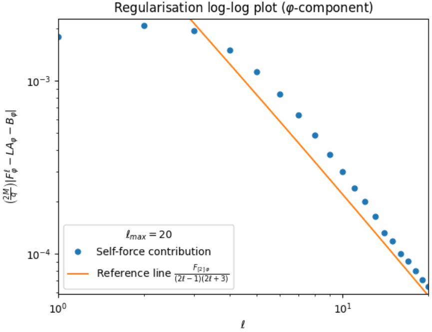

The other components also pass basic regularisation tests. These are more challenging to calculate due to low-frequency contributions.

Comparison with Oliver Long

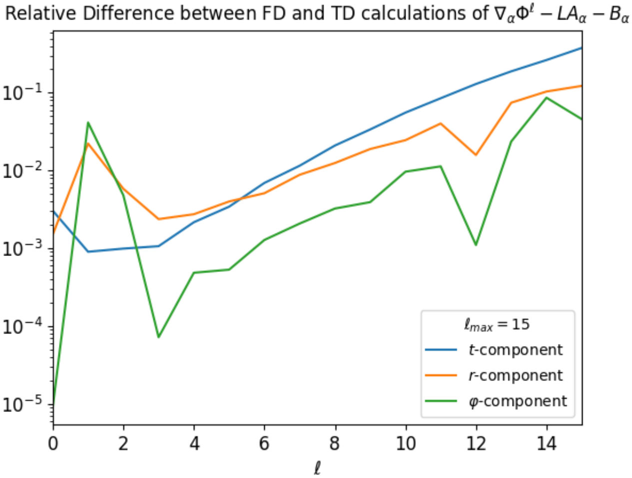

We obtain good agreement with Oliver Long's time domain code

Summary and outlook

We have:

- Developed methods to improve the convergence and runtime of the integrals $C^{-}_{\ell m\omega}$.
- Demonstrated the ability to accurately interpolate $C^{-}_{\ell m\omega}$ over frequency.
- Obtained caculations of the self-force at selected points along the orbit.

Next steps:

- Resolve remaining issues with isolated modes.
- Scatter-angle calculation.
- Other observables e.g. time delay.
- Comparisons with PM results.